Theor Chem Acc (1997) 97:289–300

Theoretical
Chemistry Accounts

Hydrogen transfer in the presence of amino acid radicals

Per E.M. Siegbahn[1], **Margareta R.A. Blomberg**[1], **Robert H. Crabtree**[2]

[1] Department of Physics, Stockholm University, P.O. Box 6730, S-113 85 Stockholm, Sweden
[2] Chemistry Department, Yale University, 225 Prospect Street, New Haven, CT 06520-8107, USA

Received: 10 February 1997 / Accepted: 11 February 1997

Abstract. Quantum chemical model studies of hydrogen transfer between amino acids in the presence of radicals have been performed using the density functional theory method B3LYP. These studies were made to investigate alternative mechanisms to the conventional electron transfer-proton transfer mechanisms. The model reactions studied are such that the net result of the reaction is a transfer of one neutral hydrogen atom. Simple models are used for the amino acids. Three different mechanisms for hydrogen transfer were found. In the first of these, a transition state with a protonated intermediate residue is found, in the second, the proton and electron take different paths and in the third, a neutral hydrogen atom can be identified along the reaction pathway. A key feature of these mechanisms is that charge separation is always kept small in contrast to the previous electron transfer-proton transfer mechanisms. It is therefore proposed that the processes normally considered as electron transfer in the biochemical literature could in fact be better explained as hydrogen atom transfer, at least in cases where a suitable hydrogen bonded chain pathway is present in the protein. The presence of such chains in principle allows the protein to define the path of net hydrogen transfer. Another important conclusion is that standard quantum chemical methods can be used to treat these mechanisms for hydrogen transfer, allowing for an accurate representation of the geometric changes during the reactions.

Key words: Hydrogen atom transfer – Electron transfer – Long-range electron transfer – Theoretical studies – Hydrogen bonding – Metalloproteins

1 Introduction

Proton transfer (PT) and electron transfer (ET) are ubiquitous in enzymatic transformations. In many cases the stoichiometry of the overall transformation illustrates this point by involving protons or electrons as substrates or products, as in hydrogenase, methane monooxygenase and the oxygen-evolving complex of Photosystem II (Eqs. 1–3).

$$H_2 \rightarrow 2H^+ + 2e^- \quad (1)$$

$$CH_4 + 2H^+ + 2e^- + O_2 \rightarrow CH_3OH + H_2O \quad (2)$$

$$2H_2O \rightarrow 4H^+ + 4e^- + O_2 \quad (3)$$

Often considered as separate steps, ET and PT have been the subjects of extensive study, both experimental and theoretical, and for ET both in coordination compounds and in proteins [1–5]. A common viewpoint is, for example, to consider the electron as coming from one part of the enzyme, while the proton can come from an entirely different part. Although the ET and PT steps are clearly viewed as coupled in the sense that they are both part of the same reaction sequence, an instantaneous coupling between the protons and the electrons is not considered to exist. Recently, modifications of the pure electron transfer viewpoint has been suggested. However, the proton coupled electron transfer (PCET) model [6] still focusses on the electron transfer picture but uses protonic motion to simplify the electron transfer. Methods similar to the ones used for pure electron transfer are used.

In experimental small molecule chemistry, hydrogen atom transfer (HAT) is a typical property of radicals. The direction of the reaction is governed by the bond strengths, so that Eq. (4) will tend to go in the forward direction if the X-H bond energy exceeds the Y-H bond energy.

$$X\cdot + YH \rightarrow XH + Y\cdot \quad (4)$$

The intrinsic barrier for HAT in the exothermic direction is small, often in the range of 2–4 kcal/mol. The reaction is essentially unaffected by solvent polarity, indicating charge separation is small or zero [7]. Experimental examples of PCET have been best demonstrated by electrochemical means, where the reactions is pH dependent, and a net H transfer proceeds by ET from the electrode coupled with PT from the electrode surface [8, 9].

Correspondence to: P.E.M. Siegbahn

In the present study, we consider reactions that go by hydrogen transfer, where the amino acid reactants and products are both neutral and only differ by the position of one hydrogen atom. One of the reactant amino acids is a radical and another one has a hydrogen atom that can be transferred. Several different model examples are considered for the hydrogen transfer. In most of these models there is also an intermediate amino acid residue, so that altogether three amino acids are present. Models considered include, for example, cases where the amino acid radical is a Σ or a II state (i.e. has the unpaired electron in a σ or a π orbital), and cases where the intermediate residue is an acid or a base. Water is also considered as a possible intermediate group. Small barriers are found for all these reactions. Three distinctly different mechanisms for hydrogen transfer are identified, all of them probably quite common in biochemical systems. Another important property of these hydrogen transfer mechanisms is that charge separation is always kept small. These processes are relevant to enzymatic processes, we believe, because, in the low dielectric medium of a protein, charge separation tends to be minimal, hence they provide an attractive mechanism for "electron transfer". An important conclusion for future work is that standard quantum chemical methods are shown to be adequate to describe these process, which can best be considered as normal chemical reactions. All the important geometric changes that occur during the hydrogen transfer can therefore be accurately handled by efficient energy gradient techniques.

2 Computational details

2.1 Methods and basis sets

The calculations on the hydrogen transfer reactions were performed in two steps. First, an optimization of the geometry was performed using B3LYP, a density functional theory (DFT) type of calculation based on hybrid functionals, and double zeta basis sets. In the second step the energy was evaluated in the optimized geometry using very large basis sets including diffuse functions and with two polarization functions on each atom. The final energy evaluation was also performed at the B3LYP level. All these calculations were performed using the GAUSSIAN-94 program [10]. In some test calculations the energy was also evaluated using a parametrized scheme, PCI-80 (parametrized configuration interaction with parameter 80) [11], based on conventional quantum chemical methods.

The present DFT calculations were made using the empirically parametrized B3LYP method [12, 13]. The B3LYP functional can be written as

$$F^{B3LYP} = (1-A) * F_x^{Slater} + A * F_x^{HF} + B * F_x^{Becke} + C * F_c^{LYP} + (1-C) F_c^{VWN}$$

where F_x^{Slater} is the Slater exchange, F_x^{HF} is the Hartree-Fock exchange, F_x^{Becke} is the gradient part of the exchange functional of Becke [12], F_c^{LYP} is the correlation functional of Lee et al. [14] and F_c^{VWN} is the correlation functional of Vosko et al. [15]. A, B, and C are the coefficients determined by Becke [12] using a fit to experimental heats of formation. However, it should be noted that Becke did not use F_c^{VWN} and F_c^{LYP} in the expression above when the coefficients were determined, but used the correlation functionals of Perdew and Wang instead [16].

The B3LYP energy calculations were made using the large 6-311 + G(2*d*,2*p*) basis sets in the GAUSSIAN-94 program. This basis set has two sets of polarization functions on all atoms, and also diffuse functions which are found to be important when interactions with oxygen-containing systems like water are studied. In the B3LYP geometry optimizations a much smaller basis set (LANL2DZ) of only double zeta quality was used. At the final geometries, Hessians were also calculated in most cases at the same B3LYP level as the geometries were determined. In some cases Hartree-Fock Hessians where the frequencies were scaled by 0.90 were used instead.

For some of the smallest of the present model systems comparative calculations were made using the PCI-80 scheme [11]. This parametrized scheme is based on calculations performed using the modified coupled pair functional (MCPF) method [17], which is a standard quantum chemical, size-consistent, single reference state method. The zeroth-order wave-functions were determined at the self-consistent field (SCF) level. When standard double zeta plus polarization (DZP) basis sets are used it has been shown that about 80% of the correlation effects on reaction energies are obtained irrespective of the system studied. A good estimate of a reaction energy is thus obtained by simply adding 20% of the correlation effects, and this is what is done in the PCI-80 scheme. The parameter 80 is thus empirical, not fitted but chosen to give agreement with experiment for a similar benchmark test as the one used for the B3LYP method. The PCI-80 calculations were performed using the STOCKHOLM set of programs [18]. Standard DZP basis sets were used in these calculations. For carbon, nitrogen and oxygen the primitive (9*s*,5*p*) basis of Huzinaga [19] was used, contracted according to the generalized contraction scheme to [3*s*, 2*p*] and one *d* function was added. For hydrogen the primitive (5*s*) basis from Ref. [19] was augmented with one *p* function and contracted to [3*s*, 1*p*].

2.2 Amino acid models

Although it is possible to treat individual amino acids using the present high accuracy quantum chemical methods, it is not yet possible to treat reactions involving several amino acids. Therefore, simpler models are needed to treat the hydrogen atom transfer reactions of present interest. Since X—H bonds are broken and formed in these reactions, the model used to mimic the enzyme should ideally have a similar X—H bond strength and proton affinity. Some X—H bond strengths and proton affinities for different amino acid models are listed in Table 1 see also Fig 1.

The O—H bond strength of tyrosine, recently calculated using the same basis set as here, was found to be

Table 1. X—H bond strengths in kcal/mol, X=O, N, C. Some proton affinities are also given

Molecule	B3LYP	PCI-80	Exp
X=O			
Tyrosine	82.2		
Phenol	83.1	85.3	86.5 ± 2
Vinyl alcohol	81.6	80.3	
Formic acid	107.5	110.4	
Methanol	99.4	102.8	104.4 ± 1
Hydrogen peroxide	82.4	85.3	88.2
Water	114.4	114.8	119 ± 1
X=N			
Formamidine	97.0	92.9	
Imidazole	92.9	92.1	
X=C			
Methane	101.5	103.5	104.8 ± 0.2
Proton affinities			
Formamidine	226.0	230.4	
Imidazole	224.0	228.3	

82.2 kcal/mol [20]. With the same resonance stabilization, phenol has a similar weak O—H bond strength of 83.1 kcal/mol. However, to model tyrosine economically a still smaller system with a similar resonance for the radical is preferable. Vinyl alcohol (Fig. 1e) with an O—H bond strength of 81.6 kcal/mol is indeed quite similar to tyrosine, and vinyl alcohol should therefore be a good model for the present purpose.

A second important amino acid to model is histidine, for which imidazole (see Fig. 1i) is obviously a good model, like phenol is a good model of tyrosine. Although fairly large, imidazole has been used in some of the present model calculations. The calculated N—H bond strength is 92.9 kcal/mol, showing that the radical resonance is less effective than for tyrosine, phenol and vinyl alcohol. Experimentally, histidine is considered as a basic amino acid found to be protonated or neutral at physiological pH, and for this reason it is even more important to model the proton affinity correctly, calculated to be 224.0 kcal/mol for imidazole. A simpler model for histidine, formamidine (see Fig. 1g), is found to have a slightly larger N—H bond strength of 97.0 kcal/mol, but the more important proton affinity of 226.0 kcal/mol is quite similar to that for imidazole. Formamidine can be considered as an even better model for arginine, which is always found to be protonated at physiological pH.

A third common amino acid important to model is glutamic acid. In the present studies glutamic acid is modeled by formic acid. The calculated O-H bond strength of formic acid, 107.5 kcal/mol, is substantially larger than that for tyrosine of 82.2 kcal/mol, showing that the radical resonance is quite ineffective in this case. Experimentally, glutamic acid is always found to be negative at physiological pH. Formic acid can also be considered as a good model for aspartic acid.

Other models, used in the present hydrogen transfer studies, were not chosen to be similar to any particular amino acid, but instead to span a range of X—H bond strengths. The calculated O—H bond strength of methanol is 99.4 kcal/mol, of hydrogen peroxide 82.4 kcal/mol and of water 114.4 kcal/mol. Finally, the B3LYP value for the C—H bond strength of methane is 101.5 kcal/mol.

2.3 Accuracy

Before the hydrogen transfer reactions are discussed in detail, the accuracy of the B3LYP method can be tested. This can be done both by comparisons to available experiments and by testing against other methods also known to have high accuracy in most cases. Results of these comparisons can be found in Tables 1 and 2.

The B3LYP X—H bond energies discussed above can first be compared to experiments. As seen in Table 1, the O—H bond strengths are systematically underestimated by 3–6 kcal/mol at the B3LYP level. Since in the reactions of present interest, one bond is formed simultaneously as another is broken, a systematic underestimation of the bond strengths by a similar amount should only have a small effect on the reaction energies. The C—H bond energy of methane is underestimated by a similar amount as are the O—H bond energies.

The bond energies obtained at the PCI-80 level are in general better than those at the B3LYP level by 2–3 kcal/mol. Comparisons to PCI-80 results should therefore be useful for calibrating the accuracy of the B3LYP method. For the X—H bond strengths not known experimentally, the B3LYP method also shows good overall agreement with the PCI-80 results: for the X—H bond strengths of phenol, vinyl alcohol, formic acid and imidazole the differences are all less than 3 kcal/mol. For formamidine the disagreement is slightly larger and in the opposite direction, but this is probably because of a slight problem in describing the radical at the PCI-80 level.

The comparisons given in Table 2 are even more relevant for the present study than the ones in Table 1. The results listed concern hydrogen transfer reactions for smaller systems than those discussed below in Sect. 3. The transfer from methane to the hydroxyl radical is exothermic by 12.9 kcal/mol at the B3LYP level and by 11.7 kcal/mol at the PCI-80 level. The barrier at the PCI-80 level is 3.0 kcal/mol, while at the B3LYP level it is zero. That the B3LYP method systematically underestimates hydrogen transfer barriers is general and has also been found recently by others [21, 22]. The underestimation can be 3–4 kcal/mol. In general, it is probably reasonable to regard the B3LYP values as lower bounds to the actual barrier heights. On the other hand, tunneling, which is not accounted for here, should have a compensating effect and lead to lower effective barriers.

A trend similar to the one discussed above for the hydroxyl radical is also obtained for hydrogen abstraction from methane by the peroxide radical. In this case the reaction is quite endothermic, by 18.0 kcal/mol at the B3LYP level and 17.0 kcal/mol at the PCI-80 level. The barrier obtained at the B3LYP level is underestimated as usual, in this case only by 1.8 kcal/mol: 20.9 kcal/mol compared to 22.7 kcal/mol at the PCI-80 level. It should be pointed out that although this appears

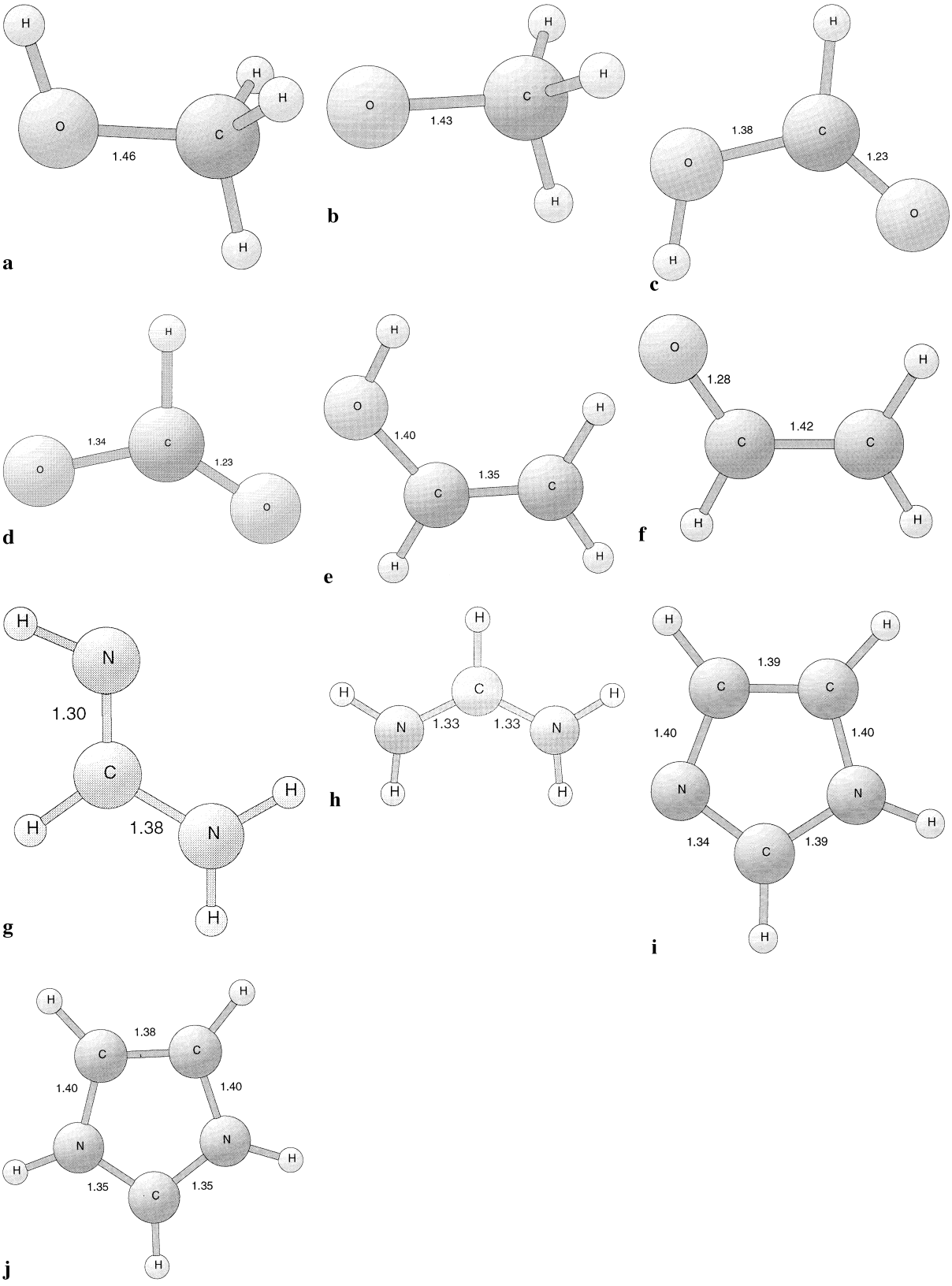

Fig. 1a–j. Geometry optimized structures of models used in the present study. The corresponding amino acid is given in parenthesis. **a** Methanol. **b** Methoxy radical. **c** Formic acid (glutamic acid). **d** Formyl radical. **e** Vinyl alcohol (tyrosine). **f** Vinyloxo radical. **g** Formamidine (arginine). **h** Protonated formamidine. **i** Imidazole (histidine). **j** Protonated imidazole

Table 2. Barriers ($\Delta E^{\#}$) and reaction energies ΔE for hydrogen atom transfer in kcal/mol

Molecular complex	B3LYP	PCI-80
HO···CH_4		
ΔE	−12.9	−11.7
$\Delta E^{\dagger}$	0.0	3.0
HOO···CH_4		
ΔE	18.0	17.0
$\Delta E^{\dagger}$	20.9	22.7
HO···H_2O		
ΔE	0	0
$\Delta E^{\dagger}$	4.2	5.0

to be a high abstraction barrier, most of it is endothermicity. In the opposite direction, the hydrogen transfer has a barrier of only 2.9 kcal/mol at the B3LYP level and 5.7 kcal/mol at the PCI-80 level.

Finally, a thermoneutral hydrogen transfer reaction was studied. Hydrogen transfer between water and the hydroxyl radical is also found to have a low barrier of 4.2 kcal/mol at the B3LYP level in very good agreement with the PCI-80 value of 5.0 kcal/mol.

In summary, the hydrogen transfer reactions described in this section have low barriers apart from possible endothermicities. These low barrier reactions are best described as hydrogen atom transfers. As will be shown below, two entirely different mechanisms for hydrogen transfer are at least as common in the model systems studied and, we propose, probably also in biochemical systems.

3 Results and discussion

In this section several model cases of hydrogen transfer are examined at the B3LYP level for systems where a hydrogen bonded amino acid radical is present. This radical was in most cases selected to be a tyrosyl radical (here modeled by vinyl alcohol) since this is the most abundant amino acid radical in biochemical systems. When the reactants and products are compared for all these model reactions, they can be described as a net transfer of one neutral hydrogen atom. These reactions can also be described as radical transfer reactions, since they transfer the neutral radical character from one amino acid to another one. From the results of these studies, the hydrogen transfer reactions can be divided into three main classes. In the first class, described in Sect. 3.1 a basic residue is protonated in the transition state. The mechanism in this reaction will be termed proton governed hydrogen transfer (PGHT), since the emphasis is on the protonated basic intermediate residue. This type of hydrogen transfer reaction is probably quite common in biochemical systems since it is quite efficient in transporting hydrogen (in biochemical literature normally referred to as electron transfer) over long distances. The second type of hydrogen transfer reaction, described in Sect. 3.2, has a separate pathway for the electron and for the proton. It requires direct overlap between orbitals on the radical and on the amino acid which is to become a radical. The mechanism in this reaction will be termed overlap governed hydrogen transfer (OGHT), since a direct overlap mechanism is involved in the hydrogen transfer. This type of hydrogen transfer may be less common in biochemical systems but can at least be clearly identified in the case of the ribonucleotide reductase (RNR) hydrogen bonded chain [23], between Tyr730 and Tyr731 (Fig. 2). Finally, in the third class there is direct HAT, in which the electron and proton being transferred stay together as a more or less neutral hydrogen atom along the entire reaction path. This type of hydrogen transfer was described in Sect. 2 for simple non-amino acid systems, but is probably a common mechanism for hydrogen abstraction in biochemical systems where a transition metal is involved. For example, this has been proposed for the mechanism of O_2 evolution in Photosystem II where a hydrogen atom is being transferred from a water molecule coordinated to manganese over to a tyrosyl radical [20, 24, 25]. Another proposed example is methane mononoxygenase (MMO) where a hydrogen atom can be abstracted from methane by an oxo group on an iron dimer complex [26–28]. It is also

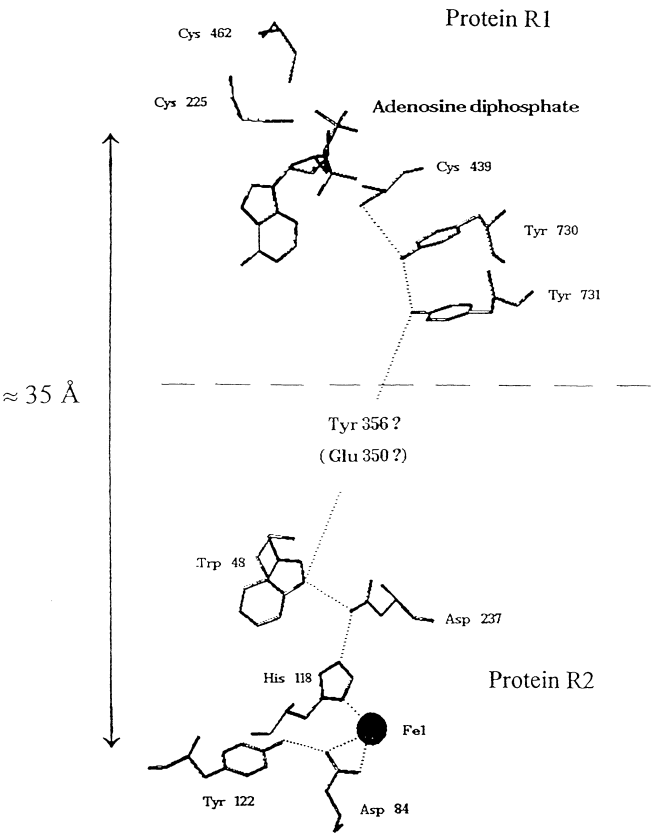

Fig. 2. Conserved residues participating in the proposed hydrogen bonded long-range transfer chain between substrate (adenine diphosphate) site in protein R1 and the tyrosyl radical in protein R2 of *E. coli* ribonucleotide reductase. The *dotted lines* represent hydrogen bonds in the crystal structures of the proteins. The *dashed line* represents the boundary between proteins R1 and R2. Tyr356 and Glu350 are not visible in the crystal structure of protein R2 because of dynamic disorder but may become ordered by interaction with R1. (Adapted from Ref. [23])

likely to be the mechanism involved where the iron dimer complex in RNR abstracts hydrogen from tyrosine [23]. All the present model reactions involving all three mechanisms have low hydrogen transfer barriers, so are realistic possibilities for hydrogen transfer in real proteins in the presence of amino acid radicals. A key property of these reactions is that they occur with small charge separations, at most on the order of 1 Å, but can affect hydrogen transfers through hydrogen bonded chains over much longer distances, possibly up to 35 Å (Fig. 2) [23]. The presence of such chains allows the protein to define the path for hydrogen transfer, and by conformational changes perhaps also to modulate its rate.

3.1 Proton governed hydrogen transfer

The first example of the type of hydrogen transfer that is here termed PGHT is shown in Figs. 3 and 4. The reactant has three amino acids linked by hydrogen bonds: tyrosine (here modeled by vinyl alcohol), then an arginine residue (modeled by a formamidine) and third the tyrosyl radical (modeled by a vinyloxo radical). The hydrogen transfer considered is the one that takes a neutral hydrogen atom from tyrosine over to the tyrosyl radical. It should be noted that the hydrogen transfer chosen was unsymmetric leading to a product that is not identical in energy to the reactant, but almost. The transition state search for this hydrogen transfer did not, as might have been expected based on the results of the previous section, converge to a concerted transition state with two simultaneous hydrogen transfers. Instead, the transition state initially found involved motion of one proton from tyrosine over to arginine. When a large basis set is used and zero-point vibrational effects are added, the energy of this structure is actually lower than the structure for a protonated arginine with two hydrogen bonded tyrosyl radicals (Fig. 4). In the protonated structure, which is thus the true transition state for the entire hydrogen transfer process, the radical electron is shared between the tyrosyl radicals and the protonic charge is spread out over the arginine. Since the Mulliken populations do not show a particularly large positive charge on any one of the hydrogen atoms, it might be argued that a hydrogen atom rather than a proton has been transferred to arginine from tyrosine. However, the geometry of the arginine intermediate residue in Fig. 3 is clearly that of Arg-H^+ (compare Fig. 1h) and not that of the neutral Arg-H radical, as was checked by calculations on these isolated systems. For example, the geometry of Arg-H is not planar while the arginine intermediate residue is planar as is the Arg-H^+ system. In fact the entire complex in Figs. 3 and 4 is planar, which makes PGHT completely different from OGHT to be described in the next subsection. The barrier for hydrogen transfer from tyrosine to tyrosyl is 5.3 kcal/mol, which is sufficiently low to make this pathway a realistic possibility in biochemical systems.

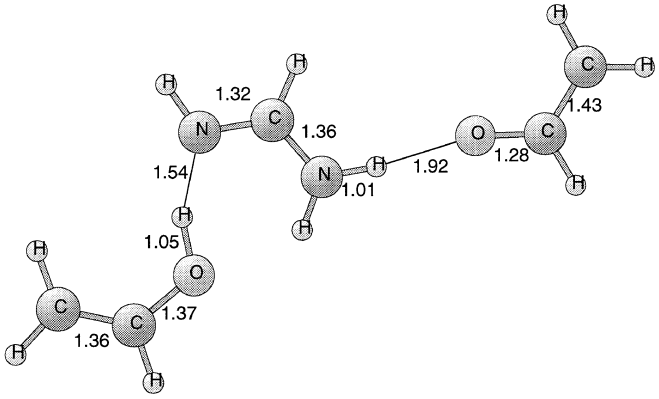

Fig. 3. The reactants for the hydrogen transfer reaction from vinyl alcohol (tyrosine) to the vinyloxo (tyrosyl) radical with formamidine (arginine) as intermediate residue

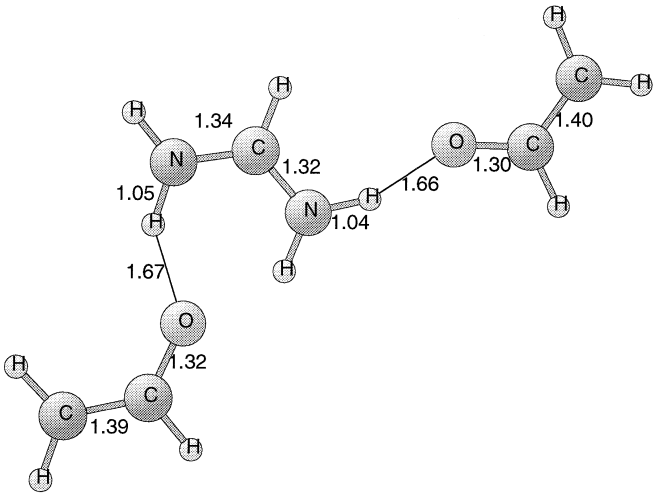

Fig. 4. The transition state for hydrogen transfer from vinyl alcohol (tyrosine) to the vinyloxo (tyrosyl) radical with formamidine (arginine) as intermediate residue. The hydrogen transfer barrier is 5.3 kcal/mol

PGHT can be described in the following way. A proton is first transferred to a basic neighboring amino acid residue. The positive charge is spread out over this residue and the compensating negative charge is very close to the positive charge located in the hydrogen bonding region. In this way costly charge separation in the relatively non-polar protein medium is kept as small as possible. The transfer of the electron does not require a direct overlap between the radical orbitals between which the electron is transferred. Instead, the electron jump is caused by successive overlapping orbitals and concerted geometric changes due to the proton transfer to the basic residue.

A few additional important points about PGHT should be emphasized. First, due to the planar nature of both reactant and transition state, PGHT is a very efficient mechanism for moving hydrogen atoms over long distances. PGHT is therefore probably the most important and common mechanism for effective hydrogen transport (earlier referred to as electron transfer) in biochemical systems where amino acid radicals are present, since one of the main purposes in these processes is to transfer hydrogens over long distances. It should, of course, be noted that it is not the same

hydrogen atom that is being transferred between the different amino acids in the chain. However, eventually a particular hydrogen atom will move along the chain in one direction in a sequence of steps leading to obvious suggestions of isotopic labeling experiments. A second important point concerns possible kinetic isotope effects (KIEs). Since the protonated transition state for the hydrogen transfer has the same number of bonds as the reactant, the KIE is expected to be close to one. This was confirmed by Hessian calculations which indicate a difference of zero-point energies of only 0.9 kcal/mol between reactant and transition state, actually with more zero-point energy for the transition state. This leads to an inverse deuterium KIE of 0.7 obtained by replacing the hydrogen being transferred between tyrosine and arginine by deuterium. Since the KIE is so close to one, this type of hydrogen transfer KIE may be difficult to observe experimentally. Another problem in this context is that the hydrogen atoms on the amino acids are exchangeable, leading to difficulties in isotopic labeling of a particular amino acid. A third point is that although charge separation is kept minimal during the hydrogen transfer in PGHT, the charge separation at the transition state is larger than for the reactants and products. This means that long-range dielectric effects are expected to lower the transfer barrier further. Studies of these effects are in progress [29].

In the hydrogen transfer described above and in Figs. 3 and 4, a proton is transferred to one of the nitrogens in arginine at the beginning of the reaction, but a proton bound to the other nitrogen leaves arginine at the end of the reaction. Another possibility is that a proton bound to the same nitrogen leaves arginine instead. As might be expected, this turns out to lead to a higher barrier. In fact, the geometry optimization failed to converge to this type of transition state but moved back to the transition state in Fig. 4. The reason for this is that the charge distribution is more favorable for the transfer in Fig. 4. With two nitrogens involved in the transfer the positive charge can be evenly distributed over arginine, but with only one nitrogen involved the charge has to be more localized around this nitrogen, since all the negative charge is in this region. Again, the charge separation is always minimized.

For the second example of PGHT, the possibility of inserting a water molecule in the hydrogen transfer chain was considered. The idea was that if water can be inserted this would be a simple way for the protein to increase the hydrogen transfer distance, since water is almost always available. The resulting transition state is shown in Fig. 5. As can be seen in this figure, the insertion of water did not actually increase the hydrogen transfer distance very much. Instead, the presence of the water molecule allows the oxygen in tyrosine to swing in and form a hydrogen bond to an N—H bond of the arginine. An interesting result of this model study is that water lowers the barrier for hydrogen transfer from 5.3 kcal/mol for the model in Figs. 3 and 4 to 3.7 kcal/mol for the model in Fig. 5. The reason for this is not that water itself is a very good hydrogen transfer agent but that there are more hydrogen bonds when water is present. Since the charge separation is larger for the transition state than for the reactant, hydrogen bonding and long-range polarization (as mentioned above) will tend to lower the hydrogen transfer barrier. This result also indicates that long-range hydrogen transfer can probably occur via a chain of residues even if some of these residues have strong O—H bonds (e.g. Ser, Thr).

In the third example of PGHT considered here, the basic intermediate arginine residue (modeled by formamidine) is replaced by histidine (modeled by imidazole). The transition state is shown in Fig. 6. The effect on the barrier of this replacement of base is a slight increase to 8.3 kcal/mol from 5.3 kcal/mol. This increase is consistent with a corresponding decrease of proton affinity of 2.0 kcal/mol (see Table 1) in going from the arginine to the histidine model. It must of course be noted in this context that there are many other effects that also influence the barrier height. The calculated KIE value of 1.8 for the case of the histidine residue is normal while that for the arginine residue was inverse. However, these KIE values are quite uncertain since there is a very strong geometric variation of the zero-point vibrational energy in the transition state region. The only really safe,

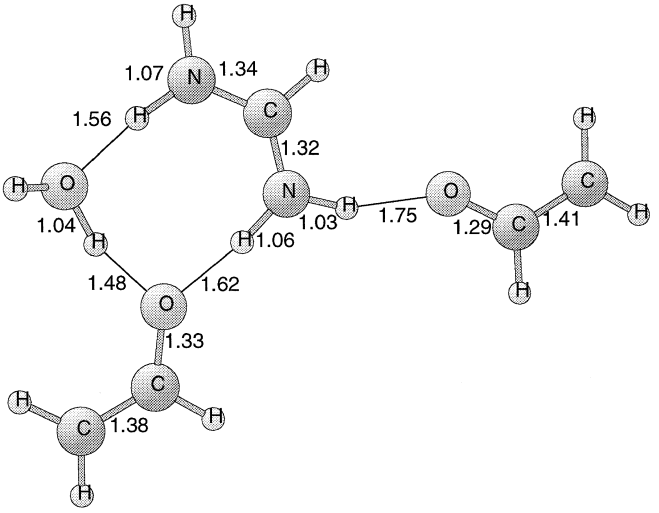

Fig. 5. The transition state for hydrogen transfer from vinyl alcohol (tyrosine) to the vinyloxo (tyrosyl) radical with formamidine (arginine) and water as intermediate residues. The hydrogen transfer barrier is 3.7 kcal/mol

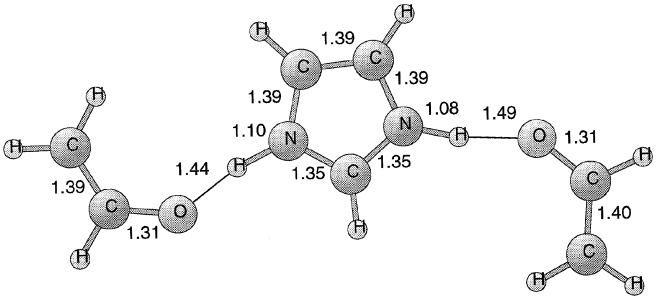

Fig. 6. The transition state for hydrogen transfer from vinyl alcohol (tyrosine) to the vinyloxo (tyrosyl) radical with imidazole (histidine) as intermediate residue. The hydrogen transfer barrier is 8.3 kcal/mol

and important, conclusion that can be drawn is that the KIE values are not large.

Another important point about the present model systems for PGHT should finally be noted. Since a different hydrogen atom is being transferred *to* the intermediate residue (arginine or histidine) than the one being transferred *from* the intermediate residue, the system does not return to the initial position without additional motion. Since, for example, in the RNR chain the hydrogens will always be transferred in the same direction, this is an important point. However, returning to the initial position after a hydrogen transfer should not be very expensive. This step will normally be slightly exothermic, but will require a rotation of the intermediate residue by 180° which may involve breaking hydrogen bonds. In order for the hydrogen transfer to work in a protein, this step just has to be faster than the time between two successive hydrogen transfers. Since this time is very long for RNR, at least on the order of 10^{-1} s, this should not be a problem in this case.

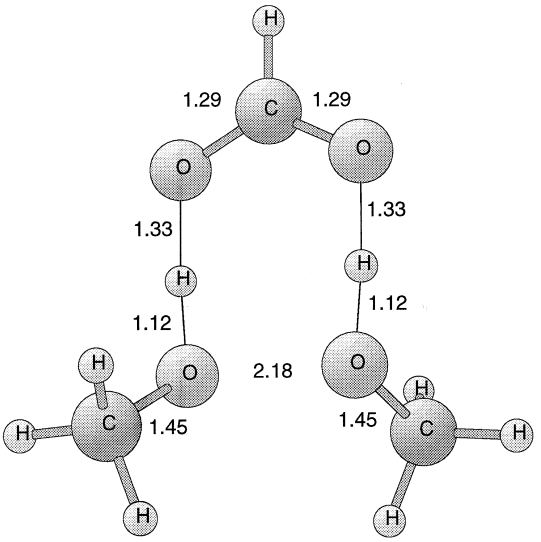

Fig. 7. The transition state for hydrogen transfer from methanol to the methoxy radical using formic acid as an intermediate residue. The hydrogen transfer barrier is 2.6 kcal/mol

3.2 Overlap governed hydrogen transfer

In some of the model studies performed for hydrogen transfer an entirely different and unexpected mechanism was encountered, here termed OGHT. This type of hydrogen transfer will be described for two different cases, for σ radicals and for π radicals.

Hydrogen transfer for the case where the radical is a Σ state (i.e. the unpaired electron is in a σ orbital) is intuitively expected to occur more easy than for II state radicals. For σ radicals, the expected type of transfer is HAT where the hydrogen atom being transferred does not change charge character more than marginally during the reaction. There is no reason for a costly separation of the proton and the electron. This picture appears to be confirmed by a model calculation for hydrogen transfer between methanol and the methoxy radical using formic acid as the intermediate molecule. The barrier for hydrogen transfer is only 2.6 kcal/mol. The quite symmetric transition state is shown in Fig. 7. This transition state has the expected appearance for an acidic intermediate residue. The O—H distances to the formyl radical are 1.33 Å, which are longer than the O—H distances of 1.12 Å to the methoxy groups. The Mulliken charge of the hydrogen atoms involved in the transport stays approximately the same during the reaction. If both hydrogens are considered to belong to the methanol groups, the intermediate formyl radical attains a negative charge of −0.54, as expected for an acidic intermediate residue. The hydrogen transfer therefore appears to be a good example of HAT. There is just one surprising feature of the transition state and this is the short O—O distance of 2.18 Å between the methoxy oxygens. Initially this short distance was rationalized by a restriction of the C—O—H angles on formic acid. It turns out that there is a quite different explanation for this distance, as will be discussed below after the next model example is presented.

The next system used to model hydrogen transfer involves π radicals as shown in Fig. 8. The π radical is

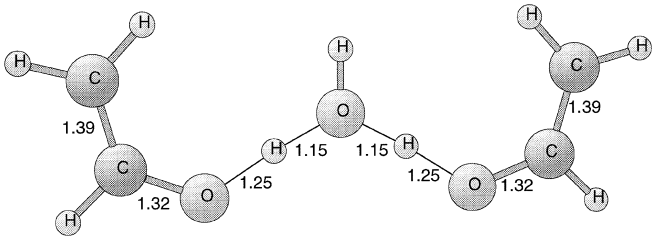

Fig. 8. The planar transition state for hydrogen transfer from vinyl alcohol (tyrosine) to the vinyloxo (tyrosyl) radical using water as an intermediate group. The hydrogen transfer barrier is 17.1 kcal/mol

chosen to be tyrosyl, here modeled by the vinyloxo radical. The intermediate group is water which could choose to be either a proton donor or a proton acceptor H-bonding group, depending on the systems involved. Since the reactants and products only differ in the position of one hydrogen atom, as in all the present model systems, and since the electron on the hydrogen atom is in the σ system, it might be expected that the transition state should be planar. However, for the planar system of Fig. 8, a surprisingly high barrier of 17.1 kcal/mol was obtained and the calculated Hessian for this planar transition state led to several imaginary frequencies and revealed that this is not a true transition state. Releasing the planar symmetry constraint led to the new transition structure shown in Fig. 9. This transition state is perfectly symmetrically placed between the reactants and products with an overall C_2 symmetry. As expected, releasing the symmetry constraint has only a minor effect for the reactants and products, so almost the whole energy change occurs for the transition state. The nonplanar reaction pathway in Fig. 9 has a much lower barrier of only 5.4 kcal/mol compared to the planar one in Fig. 8. The O—H distances in the transition state of Fig. 9 show that it is H_3O^+ rather than OH^- that is involved at the transition state. The O—H distance to the

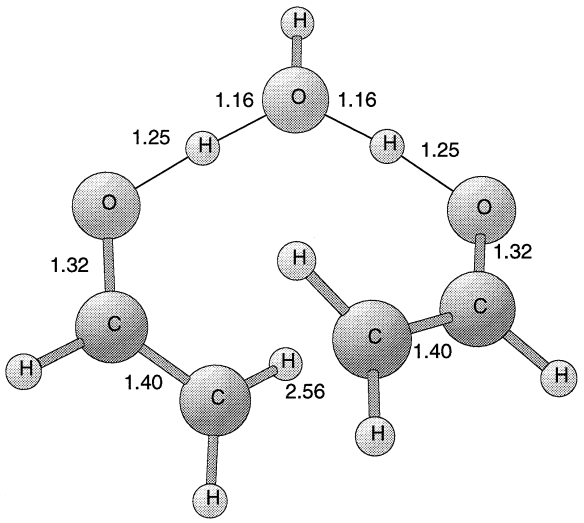

Fig. 9. The non-planar transition state for hydrogen transfer from vinyl alcohol (tyrosine) to the vinyloxo (tyrosyl) radical using water as an intermediate group. The hydrogen transfer barrier is 5.4 kcal/mol

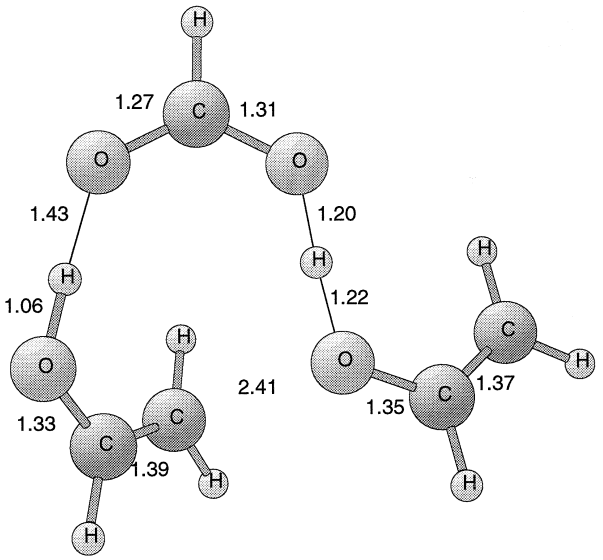

Fig. 10. The non-planar transition state for hydrogen transfer from vinyl alcohol (tyrosine) to the vinyloxo (tyrosyl) radical using formic acid (glutamic acid) as an intermediate residue. The hydrogen transfer barrier is 3.0 kcal/mol

water oxygen is 1.16 Å and to the vinyloxo groups 1.25 Å.

The explanation for the large difference in hydrogen transfer barrier for the planar and non-planar cases is initially somewhat surprising. The only logical origin for this large difference is the much smaller distance between the tyrosyl groups in the non-planar case. The shortest C—C distance is 2.56 Å. With the tyrosyl groups essentially parallel (Fig. 9), this gives some overlap between the π orbitals which are the most critical ones for the hydrogen transfer. The problem in the planar case is that the electron that is being transferred between the tyrosyl groups is a π electron, since tyrosyl is a ground state π radical, while the electron on the transferred hydrogen is a σ electron. In the OGHT mechanism the electron and the proton thus take *different paths*. The proton moves via the intermediate group, in this case water, while the electron is transferred by a direct overlap mechanism between the tyrosyl groups. The size of the hydrogen transfer barrier is apparently quite sensitive to this overlap. Since in the OGHT mechanism, the hydrogen atoms are being transferred between two atoms, the KIE is higher than in the PGHT mechanism. The calculated deuterium KIE is 2.5.

The next system used to model hydrogen transfer involving tyrosyl π radicals is shown in Fig. 10, where formic acid is used as an intermediate group, modeling a glutamic acid (or aspartic acid) residue. When this system is restricted to be planar a rather high barrier was again obtained. Releasing the planar symmetry constraint led to the transition state structure shown in Fig. 10, where the tyrosyl groups have twisted out of the plane and there is no overall symmetry. This non-planar reaction pathway has a low barrier of only 3.0 kcal/mol. The closest distance between the tyrosyl groups is 2.41 Å, similar to the 2.56 Å distance with water as an intermediate group. The O—H distances in the transition state of Fig. 10 show that glutamate, rather than glutamic acid, can be considered to be involved. The O—H distances to the formyl oxygens are 1.43 Å and 1.20 Å and to the tyrosyl groups 1.06 Å and 1.22 Å. The formyl group has a negative charge of −0.52, again consistent with the convention that the hydrogens being transferred are regarded to belong to the tyrosine groups. (If the hydrogen atom that is actually closer to the formyl group in Fig. 10 is counted as belonging to the formyl group instead, the charge on formyl is only −0.10.)

A close inspection of the transition states shown in Figs. 7, 9 and 10 shows many similarities but also some interesting differences. The structure with overlap between the oxygen σ orbitals for the methoxy groups in Fig. 7 is natural since this is a σ radical. The structure with overlap between carbon π orbitals for the tyrosyl groups in Fig. 9 is also natural, since this is a π radical. The structure with overlap between an oxygen σ and a carbon π orbital in Fig. 10 is somewhat more surprising. The reason this is a low barrier transition state is that there is some involvement of the rather low-lying tyrosyl σ radical. The σ to π transfer is the origin of the very unsymmetric transition state in Fig. 10. In fact, following the reaction path from the transition state led to different products and reactants, differing in energy by a few kcal/mol. For the lowest of these asymptotes there is a stabilizing overlap interaction of the same type as in the transition state. However, since the interaction energy is smaller than a normal hydrogen bond energy it should not be enough to keep the systems in this position. The barrier height of 3.0 kcal/mol discussed above is therefore given with respect to the asymptote without this stabilizing overlap interaction, since this is believed to be more representative of the real final states for these reactions.

A different way to utilize formic acid as the intermediate group is to transfer the hydrogens over only one of the oxygens in the formyl group. This leads to a barrier which is only slightly higher (by 1.3 kcal/mol)

than for the structure in Fig. 10. The transition state is similar to the one for water but with longer O—H distances. In the case of formic acid the O—H distances to the formyl oxygen are 1.32 and 1.31 Å, while the O—H distances in the case of water are 1.16 Å (see Fig. 9). These distances are characteristic of an acidic and a more basic intermediate group. This mechanism of using only one oxygen of the carboxylic acid in the hydrogen transfer can be seen for RNR in Fig. 2, where this is the case for Asp237. An advantage of this might be that there is less reorganization required afterwards to return to the original position.

As can be seen for the OGHT transition states, the total hydrogen transport distance is quite short. For this mechanism to be efficient for hydrogen transport over longer distances, it has to rely on the possibility of easy motion of the amino acids themselves. Indeed, if there are no other hydrogen bonds than the ones shown in the figures of the present models, the amino acids can move very easily. The OGHT reactants and products can adopt essentially planar geometries similar to those for the PGHT mechanism with only a small cost of energy (1–2 kcal/mol). A useful picture of OGHT is therefore that the amino acids swing around with large amplitudes. Occasionally, they are close enough so that there is an orbital overlap. At this point the electron and the proton can be transferred (along different paths) and the subsequent amino acid motion will lead to a hydrogen transfer over a long distance. The type of additional motion required for OGHT can be compared to that required also for PGHT to return to the initial reactant structure, discussed above in the preceding subsection.

The hydrogen transfer directly between tyrosine and tyrosyl without any intermediate residue can be regarded as a special case of OGHT. This system turns out to be quite difficult to treat computationally. The most reliable transition state is the one shown in Fig. 11. A problem here is that there is a conflict between optimal overlap and the optimal direction for the proton transfer. As discussed above, optimal overlap for this π radical

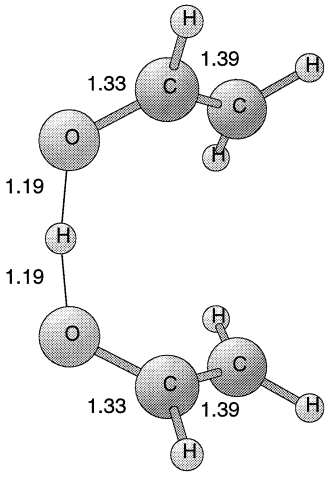

Fig. 11. The transition state for hydrogen transfer from vinyl alcohol (tyrosine) to the vinyloxo (tyrosyl) radical without any intermediate group. The hydrogen transfer barrier at the B3LYP level is 9.8 kcal/mol

should be achieved in a parallel orientation. At the transition state, this orientation requires a costly O—H bending out of the tyrosyl plane for the hydrogen being transferred. The calculated barrier is 9.8 kcal/mol, which is substantially higher than for the systems shown in Figs. 9 and 10, where the out-of-plane O—H bending is not required due to the presence of an intermediate group. Comparative calculations using other methods suggest that the calculated barrier height for this particular hydrogen transfer is very uncertain using any method. The PCI-80 barrier is, for example, 18.1 kcal/mol but this is certainly too high a value. The above value should therefore be regarded as very approximate. This situation is quite different compared to all other systems studied here and is probably due to the competition between overlap and optimal structure for hydrogen transfer. The transition state structure in Fig. 11 is quite similar to the parallel orientation of two tyrosine groups (Tyr730 and Tyr731) in the RNR chain (Fig 2). This should thus be a good example of OGHT present in a protein. It can be predicted that if there is water present this should lower the hydrogen transfer barrier at this point in the chain. Model calculations simulating hydrogen transfer in RNR are in progress [30].

The results from two additional model studies should finally be reported. In these cases the outcome of the hydrogen transfer was quite different and not relevant for biochemical systems. The first case uses the same model system as shown in Fig. 7, but a quite different transition state than the one shown in this figure was found. This second transition state also involves (apart from the hydrogen transfers shown in Fig. 7) a hydrogen transfer from the methyl group in methanol to the oxygen of the methoxy radical. This type of reaction could occur in organic radical chemistry in general, but will not occur in biochemical systems involving amino acids. This result is thus just an artifact of the models used. In the second case, two water molecules were placed as intermediate groups between a vinyl alcohol and a vinyloxo radical. In this case a C—C bond was formed between the ends of the vinyl groups. Again, such a bond could not develop in actual amino acids.

4 Conclusions

Different mechanisms for hydrogen transfer between amino acids where a radical is present have been investigated. Three different mechanisms have been identified. In the first mechanism, here termed PGHT an initial motion of a proton is critical. This proton is transferred over to a basic intermediate residue like histidine or arginine, leading to a quite symmetric planar transition state complex where the positive charge is spread out over the protonated intermediate and the negative charge is on both amino acid radicals. Both the positive and the negative charges are located close to the hydrogen bonding region and are therefore not very far removed from each other. A large charge separation is thus avoided. Since the transition state is planar, this hydrogen transfer can effectively transport hydrogen atoms over long distances in one step.

The second mechanism for hydrogen transfer is termed OGHT and in this case an orbital overlap is critical. This overlap occurs between an orbital of the amino acid radical and an orbital on the amino acid which is to become a radical. The characteristic feature of this mechanism is that the electron and the proton take different pathways. The electron goes through the overlapping orbitals, while the proton is transferred via the intermediate amino acid. Several possible overlap types have been identified with overlap between two σ orbitals, between two π orbitals and between a σ and a π orbital. An important function of the intermediate group will in this case be to minimize geometric constraints, which would otherwise be imposed on the reaction. Since overlap is required, this hydrogen transfer step does not directly lead to hydrogen atom transport over long distances. Instead, longer distance hydrogen transport in this step can be obtained by subsequent motions of the amino acids once the transfer has taken place. As before, the charge separation is kept small also for the OGHT mechanism.

The third mechanism for hydrogen transfer is HAT where the transferred proton and electron stay together as a hydrogen atom during the entire transfer reaction. This type of transfer is common in small molecule chemistry where radicals are present, but probably also occurs in biochemical systems, for example, in hydrogen abstraction reactions involving transition metal complexes. This is thus a mechanism proposed for hydrogen abstraction by the manganese cluster in PSII, and by the iron dimer complexes in RNR and in MMO.

This work shows that a suitable chain of hydrogen bonded groups can provide a low activation energy pathway for hydrogen atom transfer. Since hydrogen atom transfer can be considered as the simultaneous transfer of an electron and a proton, this mechanism also provides a pathway for electron transfer (ET). It is particularly suited for ET in proteins because the low dielectric medium of a protein makes it favorable to avoid the large charge separations unavoidable in pure ET. A picture of hydrogen transport in the presence of amino acid radicals that emerges from the present model study could be the following. HAT occurs by a sequence of individual steps. These individual steps could involve two or three amino acids of which one is a radical, as in the present model studies, or possibly more amino acids in extreme cases. It does not seem likely or necessary to involve more amino acids in each individual step of hydrogen transfer, however. Most importantly, a concerted motion of all the hydrogen atoms along an entire chain in one step is not necessary. The probability of finding a particular amino acid in a hydrogen bonded chain as a radical at a given time will then be the result of a coupling of the kinetics of these individual reactions. Eventually, at thermodynamic equilibrium, the probability for a particular amino acid in the chain being a radical should depend mainly on its thermodynamic stability. The direction of hydrogen transfer is expected to be decided by the X—H bondstrengths of the first and last members of the chain, the hydrogen atom acceptor and the hydrogen atom donor. While the hydrogen atom donor should have a weak X—H bondstrength to facilitate loss of the hydrogen atom, the intermediate hydrogen atom carriers do not have to have weak X—H bonds, as shown in this work by successful incorporation of waters as intermediate hydrogen atom carriers. In the hydrogen bonded RNR chain in Fig. 2 the most stable radical should be Cys439, which will therefore obtain radical character when needed. After the Cys439 amino acid, Tyr122 is probably the most stable radical since it has been observed experimentally. Because the hydrogen bonded chain undergoes rearrangement on hydrogen atom transfer, a subsequent rearrangement must take place before the system returns to its original state and becomes competent to transfer another hydrogen atom in the same direction as the first. Whether this picture of hydrogen transfer is correct and for which systems it applies can only be demonstrated by future experiments and it is hoped that these model studies will stimulate experiments in this direction.

One of the most important conclusions from a theoretical perspective that can be drawn from the present model studies is that standard quantum chemical methods can be used to study these reactions. This must be considered a very important point since previously, quite different and much more complicated techniques [31] were believed to be required. The major advantage of using standard quantum chemical techniques is that the very important geometric changes that occur during the reactions can be accurately obtained using gradient techniques. It is very hard to imagine that quantitatively reliable assumptions of structural changes, as required by other techniques, can in fact be made concerning these complicated reactions.

Acknowledgements. P.S. gratefully acknowledges very interesting and illuminating discussions with Astrid Gräslund and Britt-Marie Sjöberg concerning the RNR protein.

References

1. Endicott JF (1994) In: Encyclopedia of inorganic chemistry. Wiley, New York, p 1081
2. Winkler JR, Gray HB (1992) Chem Rev 92:369
3. Cannon RD (1990) In: Encyclopedia of inorganic chemistry. Wiley, New York, p 1098
4. Marcus RA (1986) J Phys Chem 90:3460
5. Walsh C (1979) Enzymatic reaction mechanisms. Freeman, San Francisco
6. Cukier RI (1994) J Phys Chem 98:2377
7. Perkins MJ (1994) Radical chemistry. Ellis Horwood, London
8. Cabaniss GE, Diamantis AA, Murphy WR, Linton RW, Meyer TJ (1985) J Am Chem Soc 107:1845
9. Thorp HH, Sarneski JE, Brudvig GW, Crabtree RH (1989) J Am Chem Soc 111:9249
10. Frisch MJ, Trucks GW, Schlegel HB, Gill PMW, Johnson BG, Robb MA, Cheeseman JR, Keith TA, Petersson GA, Montgomery JA, Raghavachari K, Al-Laham MA, Zakrzewski VG, Ortiz JV, Foresman JB, Cioslowski J, Stefanov BR, Nanayakkara A, Challacombe M, Peng CY, Ayala PY, Chen W, Wong MW, Andres JL, Replogle ES, Gomperts R, Martin RL, Fox DJ, Binkley JS, Defrees DJ, Baker J, Stewart JP, Head-Gordon M, Gonsales C, Pople JA (1995) GAUSSIAN 94 (revision A.1) Gaussian, Inc., Pittsburgh, Pa
11. Siegbahn PEM, Blomberg MRA, Svensson M (1994) Chem Phys Lett 223:35; Siegbahn PEM, Svensson M, Boussard PJE (1995) J Chem Phys 102:5377

12. Becke AD (1988) Phys Rev A38:3098; Becke AD (1993) J Chem Phys 98:1372; Becke AD (1993) J Chem Phys 98:5648
13. Stevens PJ, Devlin FJ, Chablowski CF, Frisch MJ (1994) J Phys Chem 98:11623
14. Lee C, Yang W, Parr RG (1988) Phys Rev B37:785
15. Vosko SH, Wilk L, Nusair M (1980) Can J Phys 58:1200
16. Perdew JP, Wang Y (1992) Phys Rev B 45:13244; Perdew JP (1991) In: Ziesche P, Eischrig H (eds) Electronic structure of solids. Akademie Verlag, Berlin; Perdew JP, Chevary JA, Vosko SH, Jackson KA, Pederson MR, Singh DJ, Fiolhais C (1992) Phys Rev B 46:6671
17. Chong DP, Langhoff SR (1986) J Chem Phys 84:5606
18. STOCKHOLM is a general purpose quantum chemical set of programs written by Siegbahn PEM, Blomberg MRA, Pettersson LGM, Roos BO and Almöf J
19. Husinaga S (1965) J Chem Phys 42:1293
20. Blomberg MRA, Siegbahn PEM, Styring S, Babcock GT, Åkermark B, Korall P J Am Chem Soc. (in press)
21. Durant JL (1996) Chem Phys Lett 256:595 (in press)
22. Jursic BS (1996) Chem Phys Lett 256:603
23. Sjöberg BM (1994) Structure 2:793
24. Hoganson CW, Lydakis-Simantiris N, Tang X-S, Tommos C, Warncke K, Babcock GT, Diner BA, McCracken J, Styring S (1995) Photosynth Rest 46:177
25. Tommos C, Tang X-S, Warncke K, Hoganson CW, Styring S, McCracken J, Diner BA, Babcock GT (1995) J Am Chem Soc 117:10325
26. a) Lipscomb JD (1994) Annu Rev Microbiol 48:371; b) Nesheim JC, Lipscomb JD (1996) Biochemistry 35:10240 and references cited therein
27. Feig AL, Lippard SJ (1994) Chem Rev 94:759
28. Siegbahn PEM, Crabtree RH (1997) J Am Chem Soc 119:3103
29. Pavlov M, Blomberg MRA, Siegbahn PEM (work in progress)
30. Eriksson L, Himo F, Siegbahn PEM, Gräslund A (work in progress)
31. Newton M (1991) Chem Rev 91:767